

Coherent backscattering of a picosecond pulse from a disordered medium: Analysis of the pulse shape in the time domain

K. M. Yoo, K. Arya,* G. C. Tang, Joseph L. Birman, and R. R. Alfano

*Institute for Ultrafast Spectroscopy and Laser, Photonic Application Laboratory, Department of Physics,
The City College of New York, New York, New York 10031*

(Received 16 June 1988; revised manuscript received 10 January 1989)

We have studied the temporal profile of the picosecond laser pulse scattered from random media in the backward direction in two angular regions: coherent ($-1 \leq \theta \leq 1$ mrad) and diffuse ($7.5 \leq \theta \leq 9.5$ mrad), using a streak camera with overall 15-ps time resolution. To give a good description of the temporal profile of the scattered pulse, in addition to a diffusion term, terms from the maximally crossed diagrams are required to account for the coherent enhancement of scattered intensity in the backward direction due to time-reversal symmetry.

Recently, there has been growing interest in studies of multiple scattering and Anderson localization¹⁻⁶ of electromagnetic waves in a random medium. Anderson localization is due to the coherent interference between waves scattered from random scatterers, which causes the transmission coefficient to vanish. Although Anderson localization has not yet been observed in transmission experiments, a weak coherent interference effect⁷⁻¹⁸ has been observed in scattering experiments. These experiments were performed using a cw laser incident on random media which consist of concentrated latex beads dispersed in water, and the scattered intensity in the exact backward direction was found to be about twice the diffused scattered intensity. This effect is due to the time-reversal symmetry in the scattering process of the waves in random media. Corresponding to any given path of wave propagation in the medium, there is always another wave propagating in reversed time direction. These two counterpropagating waves maintain some phase correlation even in a random medium. For example, one can easily show that these two waves have exactly the same phase when they are counterpropagating along the same path in space. Therefore, for scattering in the exact backward direction, their amplitudes add coherently to give an increased intensity which is a factor of 2 greater than the scattered intensity in other directions (diffuse scattering). The angular width of the coherent peak, or the increase in intensity at other angles close to the backward direction, depends on the phase correlation between the counterpropagating waves in the random medium.

Time-reversal symmetry holds for photon transport as well as for electron transport as long as the symmetry is not destroyed along the scattering paths. Thus, study of the transport of the former would also lead to understanding of the transport of the latter. The real time dynamics of electron transport in a random medium due to weak localization alone is difficult to probe experimentally. However, this problem can be illuminated by studies of the real time dynamics of photon transport which can be conveniently probed by an ultrafast laser with streak camera detection. The understanding of the effect of weak localization on the real time reflection of photon and electronic pulses from random media is important, particularly because

of the current advances in the applications of ultrafast photon and electronic pulses. Although the reflection of a light pulse from a random medium has been studied before,¹⁹ the effect of weak localization on the scattered pulse time profile has not been taken into account. In this paper, the temporal profile of intensity of the reflected pulse from the random media backscattered in two angular cones, one making an angle from -1.0 to 1.0 mrad and the other from 7.5 to 9.5 mrad, were measured with a streak camera and analyzed theoretically.

In our experiments, we studied the scattering of a ps (10^{-12} s) pulse from latex beads dispersed in water which was contained in a $1 \times 1 \times 5$ -cm⁻¹ glass cell. The latex bead concentration in water was 10% and studies were carried out on various bead diameters of 0.09, 0.46, 0.6, 1.06, and 16.8 μ m. A schematic of the experimental setup is shown in Fig. 1. A 15-ps/530 nm pulse was generated from a Nd mode-locked-glass and potassium diphosphate (KDP) laser system. The laser pulse was collimated by two pinholes and incident on the random medium after reflecting from a 50%-50% beam splitter. Light scattered in the backward direction was collected by a converging lens and focused onto the detector of the streak camera. The slit of the detector was placed at the focal plane of the lens, so that the light scattered into each angle would fall onto a corresponding region of the detector. Two detection windows were set on the streak camera, the first window measured the intensity of backscattered light making

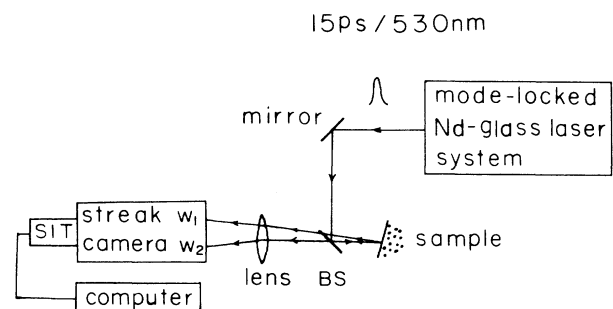


FIG. 1. Schematic of experimental setup. BS denotes beam-splitter.

an angle between -1 and 1 mrad (coherent region), while the second window measured the intensity of the light scattered between 7.5 and 9.5 mrad (diffusive region). The scattered-pulse profile from a single shot showed a rather noisy characteristic which is typical of multiple scattering from random media. A smooth profile was obtained when an average of 30 measurements were taken.

Figure 2 shows the intensity profile in the time domain for the incident laser pulse and the scattered pulse in the coherent region from two different random media. The actual intensity of scattered light in the backward direction is much weaker than the incident pulse. However, the peaks of the scattered pulses were normalized to the peak of the laser-pulse intensity for comparison of the pulse profiles scattered from the random media with different transport mean free paths. Curve 2 displays the backscattered-pulse profile from a random medium with 10% latex beads of diameter $1.06 \mu\text{m}$ dispersed in water. The transport mean free path of this medium is about $30 \mu\text{m}$. In contrast, curve 3 displays the backscattered pulse profile from a medium with beads of diameter $0.09 \mu\text{m}$ which has a longer transport mean free path l . Both curves 2 and 3 show a similar long-tail feature which indicates that the light still is being scattered in the backward direction long after the incident pulse has ceased. The scattered light at 100 ps has probably gone through about 750 scattering events. This is computed for the case of 10% latex beads of diameter $1.06 \mu\text{m}$, where the transport mean free time is $\frac{4}{3} \times 10^{-13}$ s. There are two noticeable

differences between the scattered pulses from these two media. The peak of the scattered pulse is displaced further for media with larger l . Also, the scattered-pulse shape is fatter for media with larger l . An interesting point worth noting here is the backscattered-pulse profile from 10% concentration of latex beads with diameter of $15.8 \mu\text{m}$ is very similar to its counterpart with diameter of $0.09 \mu\text{m}$. Presumably they have the same l ,¹⁷ although the scattering characteristic of these two individual particles are very different because of their sizes compared to the wavelength. The waves will be scattered in all directions by the small particle (diameter $d < \lambda$) as for latex beads with $d = 0.09 \mu\text{m}$, whereas the waves are scattered mainly in the forward direction by a large particle ($d > \lambda$) as for $d = 15.8 \mu\text{m}$. Physically, a transient-pulse incident on a random dielectric undergoes multiple scattering during its propagation into the medium. During each scattering event, part of it also gets scattered back outside the medium. Thus, along with the diffusion of the incident pulse into the medium, we also have a reflected pulse. The intensity and the shape of the reflected pulse depends on the normalized diffusion coefficient.

The scattered light in the coherent region ($-1 \leq \theta \leq 1$ mrad) and the diffuse region ($7.5 \leq \theta \leq 9.5$ mrad) are compared in Fig. 3. It is clear from the curves that the intensity of the scattered pulse in the coherent region is higher than the diffuse region. This indicates that more photons are scattered into the coherent region and is particularly obvious in the first 40 ps. At later times, the two scattered pulses seem to merge together. The time can be

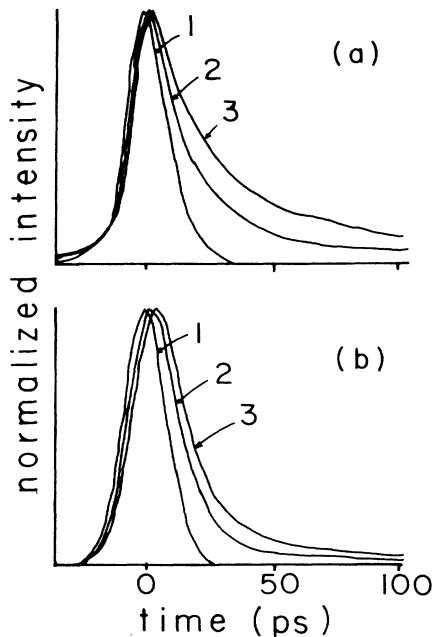


FIG. 2. The backscattered intensity vs time of ps pulse incident on random media in the coherent region ($-1 \leq \theta \leq 1$ mrad). (a) Experiment results (average of 30 shots): curve 1 incident laser pulse; curve 2 10% of latex beads of diameter $d = 1.06 \mu\text{m}$ dispersed in water; curve 3 same as 2 but $d = 0.09 \mu\text{m}$. (b) Theoretical plots: curve 1 incident laser pulse; curve 2 transport mean free path $l = 100 \mu\text{m}$; curve 3, $l = 300 \mu\text{m}$.

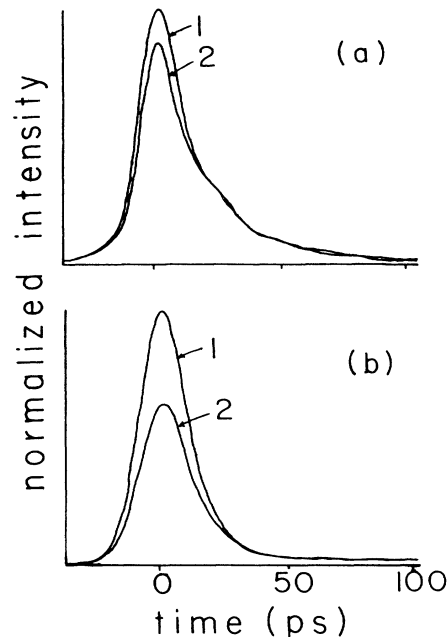


FIG. 3. The scattered intensity vs time of a ps pulse incident on a random medium, the scattered pulse in the coherent region ($-1 \leq \theta \leq 1$ mrad) and diffuse region ($-7.5 \leq \theta \leq 9.5$ mrad). (a) Experimental results from 10% latex beads with diameter of $0.46 \mu\text{m}$ dispersed in water; (b) theoretical plots with $l = 100 \mu\text{m}$.

directly related to the distance traveled by the scattered light in the random media. Thus, the constructive interference due to the time-reversal symmetry for the light scattered in the backward direction gradually diminishes at later times, and its intensity becomes equal to the diffuse intensity. A detailed analysis of the angular line shape of the coherent peak shows that the width of the line narrows as the light undergoes a longer scattering path.¹⁴⁻¹⁶ This narrowing of coherent peak can account for the two curves shown in Fig. 3(a) to merge together at later times.

Theoretically, the intensity of the scattered light in the direction \hat{s} is

$$I(\hat{s}, t) = \int dt' R(\hat{s}, t') I_0(t - t'), \quad (1)$$

where $I_0(t - t')$ is the incident pulse, and $R(\hat{s}, t')$ is the response function of the random medium. In the diffusion approximation, one can write¹¹

$$R(\hat{s}, t') = \alpha \frac{1}{\sqrt{2\pi}} e^{D_0 t'/2l} D_{-3} \left[2D_0 \frac{t'}{l^2} \right], \quad (2)$$

where α is some constant, l is the transport mean free path, $D_{-3}(x) = u(\frac{x}{2}, x)$ is the parabolic cylinder (Weber) function,²⁰ $D_0 = cl/3$ is the diffusion constant, and c is the effective speed of the wave in the medium. Equation (2) corresponds to diffuse scattering and is independent of the scattering angle. Theoretically, it corresponds to the sum of ladder diagrams in the calculation of a two-photon Green's function. To include coherent interference due to time-reversal symmetry in the scattering process, one should take the maximal crossed diagrams into account.^{11,12} The sum of the maximal crossed diagrams will result in a factor of $e^{-D_0 q^2 t'}$ in Eq. (2), where $q = (2\pi/\lambda) \times \sin\theta$, and θ is the angle \hat{s} made with the backward direction of the incident light. This term accounts for the coherent interference between scattered waves propagating in the time-reversed path in the random medium, and exhibits the following important characteristics. The intensity at $\theta=0$ is highest and is a factor of 2 greater than the diffusive intensity ($\theta=0$ corresponds to the exact backward direction); and the contribution of coherent intensity enhancement diminishes with larger t' which corresponds to longer scattering path lengths. The final expression for the intensity of the scattered pulse is

$$I(\hat{s}, t) = \alpha \frac{1}{\sqrt{2\pi}} \int dt' R(\hat{s}, t') (1 + e^{-D_0 q^2 t'}) I(t - t'). \quad (3)$$

If the random medium is absorbing with coefficient γ , then an absorption factor of $e^{-\gamma t}$ should be included in the integrand of Eq. (3). However, within the time scale of less than 100 ps in which we are working, the absorption from the latex beads can be safely neglected.

The intensity of the scattered light in the direction \hat{s} can

be computed numerically from Eq. (3). Figure 2(b) shows the theoretical plots of the incident pulse, and the scattered pulses in the backward direction (integrating θ between -1 and $+1$ mrad) from two different random media with transport mean free paths of 100 and 300 μm . These plots show characteristics similar to the experimental results shown in Fig. 2(a).

Figure 3(b) displays the computed profiles of the scattered pulses in the coherent ($-1 \leq \theta \leq 1$ mrad) and diffusive regions ($7.5 \leq \theta \leq 9.5$ mrad) from a medium with transport mean free path of 100 μm . These theoretical plots also show similar salient features observed in the experiments. However, we find that the relative intensity of the coherent region to the diffuse region is larger in the theoretical plots than the experimental one. The reason is that we use scalar theory which predicts⁵⁻⁷ the intensity of the coherent peak is twice the intensity of the background. In the actual experiment where no polarizer was used, the intensity of the coherent peak is about 1.6 times the background (for latex beads with the diameter in the range of the laser wavelength). If this smaller factor is taken into account, then our theory gives closer agreement to the experimental data. In addition, we found that the theoretical curves predict faster decay than the experimental results. It is unlikely this is due the usual resolution of the streak camera and laser pulse (15 ps) used in the experiments. The most likely cause is the effect of the collecting lens which not only resolves the angular direction of the scattered light along the horizontal slit of the streak camera, but the vertical distribution of the scattered light couples with the finite width of the slit (30 μm) which could affect the temporal resolution of the streak camera. The correlation between latex bead distribution which has been neglected in theory may also effect the pulse shape.

In conclusion, the phenomenon of weak localization in real time has been observed in the ps time domain. The theory for the temporal profile of the backscattered pulse has been formulated in the diffusion approximation, and terms from the maximal crossed diagrams are required to account for the coherent backscattering. This formulation gives a good description of the experimental results where the scattered-pulse profile is characterized by l and θ .

Note added: A theoretical result similar to our Eq. (3) was independently obtained and recently reported by Akkermans *et al.* [J. Phys. (Paris) **49**, 77 (1988)].

We thank the Hamamatsu Photonic Company and Strategic Defense Initiative for support of this research. K. M. Y. would like to acknowledge support of the Physics Department of the City College, and the Graduate Center of the City University of New York. J. L. B. received partial support from the Naval Air System Command Contract No. MDA-903-86-C-0181. We also thank Michael J. Stephen for helpful discussions.

*Present address: Physics Department, San Jose State University, San Jose, CA 95012.

¹Sajeev John, Phys. Rev. Lett. **53**, 2169 (1984).

²Ping Sheng and Zhao-Qing Zhang, Phys. Rev. Lett. **57**, 1879 (1986).

³K. Arya, Z. B. Su, and Joseph L. Birman, Phys. Rev. Lett. **57**, 2725 (1986).

⁴Sajeev John, Phys. Rev. Lett. **58**, 2486 (1987).

⁵Ping Sheng, Zhao-Qing Zhang, Benjamin White, and Georg Papanicolaou, Phys. Rev. Lett. **57**, 1000 (1987).

- ⁶Benjamin White, Ping Sheng, Zhao-Qing Zhang, and Georg Papanicolaou, *Phys. Rev. Lett.* **59**, 1918 (1987).
- ⁷Y. Kuga and A. Ishimaru, *J. Opt. Soc. Am.* **8**, 831 (1984).
- ⁸Meint P. Van Albada and Ad Lagendijk, *Phys. Rev. Lett.* **55**, 2692 (1985).
- ⁹Pierre-Etienne Wolf and Georg Maret, *Phys. Rev. Lett.* **55**, 2696 (1985).
- ¹⁰E. Akkermans, P. E. Wolf, and Maynard, *Phys. Rev. Lett.* **56**, 1471 (1986).
- ¹¹Michael J. Stephen and Gabriel Cwilich, *Phys. Rev. B* **34**, 7564 (1986).
- ¹²Michael J. Stephen, *Phys. Rev. Lett.* **56**, 1809 (1986).
- ¹³M. Rosenbluh, I. Edrei, M. Kaveh, and I. Freud, *Phys. Rev. A* **35**, 4458 (1987).
- ¹⁴Meint P. Van Albada, Martin B. van der Mark, and Ad Lagendijk, *Phys. Rev. Lett.* **58**, 361 (1987).
- ¹⁵S. Etemad, R. Thompson, M. J. Andrejco, Sajeev John, and F. C. Mackintosh, *Phys. Rev. Lett.* **59**, 1420 (1987).
- ¹⁶K. M. Yoo, Y. Takiguchi, and R. R. Alfano (unpublished).
- ¹⁷G. H. Watson, Jr., P. A. Fleury, and S. L. McCall, *Phys. Rev. Lett.* **58**, 945 (1987).
- ¹⁸A. Z. Genack, *Phys. Rev. Lett.* **58**, 2043 (1987).
- ¹⁹A. Ishimaru and K. J. Painter, *Radio Sci.* **15**, 87 (1980).
- ²⁰M. Abramowitz and I. A. Stegun, *Handbook of Mathematical Functions* (Dover, New York, 1960), p. 686.